

Topological Optimization of Structures Using a Multilevel Nodal Density-Based Approximant

Yu Wang¹, Zhen Luo^{1,2} and Nong Zhang¹

Abstract: This paper proposes an alternative topology optimization method for the optimal design of continuum structures, which involves a multilevel nodal density-based approximant based on the concept of conventional SIMP (solid isotropic material with penalization) model. First, in terms of the original set of nodal densities, the Shepard function method is applied to generate a non-local nodal density field with enriched smoothness over the design domain. The new nodal density field possesses non-negative and range-bounded properties to ensure a physically meaningful approximation of topology optimization design. Second, the density variables at the nodes of finite elements are used to interpolate elemental densities, as well as corresponding element material properties. In this way, the nodal density field by using the non-local Shepard function method is transformed to a practical elemental density field via a local interpolation with the elemental shape function. The low-order finite elements are utilized to evaluate the displacement and strain fields, due to their numerical efficiency and implementation easiness. So, the proposed topology optimization method is expected to be efficient in finite element implementation, and effective in the elimination of numerical instabilities, e.g. checkerboards and mesh-dependency. Three typical numerical examples in topology optimization are employed to demonstrate the effectiveness of the proposed method.

Keywords: Topology optimization, SIMP, Shepard function, Numerical instabilities

1 Introduction

In the area of structural optimization, topology optimization has experienced considerable development over the past two decades with a wide range of engineering

¹ School of Electrical, Mechanical and Mechatronic Systems, The University of Technology, Sydney, NSW 2007, Australia

² Corresponding Author. Tel: +61-2-9514 2994; Fax: +61-2-9514 2655. E-mail address: zhen.luo@uts.edu.au

applications [Bendsøe and Sigmund (2003)]. Topology optimization is essentially a systematic design methodology, which involves a numerical process to iteratively re-distribute a given amount of material inside the design domain subject to loads and boundary conditions, until a prescribed design objective is optimized under specified design constraints. Topology optimization has been recognised as the most promising but the most challenging approach in the conceptual stage of structural optimization. Many different methods have been developed for topology optimization of structures, including the homogenization method [Bendsøe and Kikuchi (1988)], SIMP method [Zhou and Rozvany (1991); Mlejnek (1992); Bendsøe and Sigmund (1999)], and level set-based methods [Sethian and Wiegman (2000); Wang, Wang and Guo (2003); Allaire, Jouve and Toader (2004); Luo, Wang, Wang and Wei (2007)]. It is noted that there are also many alternative topology optimization methods, such as meshless methods-based topology optimization of structures [e.g. Li and Atluri (2008); Zheng, Long, Xiong and Li (2008); Luo, Zhang, Gao and Ma (2012)], and a physically meaningful level-set based topology optimization [Luo, Zhang and Wang (2012)].

Topology optimization of continuum structures essentially belongs to a set of integer programming problems with a large number of discrete (0, 1) design variables. More efficient gradient-based optimization algorithms cannot be directly applied to solve such large-scale optimization problems due to the well-known combinatorial problem. To this end, the homogenization and SIMP methods have been widely employed to relax the discrete topology optimization problem, allowing the design variables taking intermediate densities from 0 and 1. In doing so, the original optimization problem is changed to a regularized optimization problem with range-bounded continuous design variables. In particular, the SIMP, as an extension of the homogenization method, has won great popularity in topology optimization of solid mechanics problem, due to its conceptual simplicity and implementation easiness. In SIMP-based topology optimization methods, a ‘power-law’ criterion [Bendsøe and Sigmund (1999)] is usually applied to penalize the intermediate densities of elements, to ensure the solution of the regularized 0-1 design close to the original binary (0,1) design as much as possible. In addition, numerical schemes, for example, the filtering schemes [Sigmund (2001); Bourdin (2001); Luo, Chen, Yang, Zhang and Abdel-Malek (2005)] are required to be incorporated to eliminate numerical instabilities, e.g. the checkerboards and mesh-dependence [Diaz and Sigmund (1995); Sigmund and Petersson (1998)], in order to make a physically meaningful solution for topology

It can be found that most of the current SIMP approaches are based on element-wise design variables [Bendsøe and Sigmund (2003)], which means that both the topological geometry of material distribution and the physical fields would be eval-

uated via elemental density variables which are piecewise constant. In topology optimization of continuum structures, the element-wise variables may be one of the reasons for the occurrence of numerical instabilities [Diaz and Sigmund (1995); Sigmund and Petersson (1998)], including checkerboards, local minima, and mesh-dependency. Moreover, the element-based topology optimization method may lead to zigzag non-smooth boundary.

As a result, to overcome the shortcomings of conventional element-wise SIMP methods, several alternative methods have been proposed. More recently, there have been several approaches based on point-wise design variables [Rahmatalla and Swan (2004); Matsui and Terada (2004); Guest, Prevost, Belyschko (2004); Paulino and Le (2009); Kang and Wang (2011)]. According to these approaches, the density variables at the nodes of finite elements are normally considered as the design variables, and subsequent element material properties are obtained in terms of nodal densities via interpolation schemes. For instance, Rahmatalla and Swan (2004) proposed several options to implement the point-wise interpolation for material density fields, although “layering” or “islanding” type numerical instabilities occurred in the design. Matsui and Terada (2004) studied a so-called CAMD (continuous approximation of material distribution) method based on the homogenization method, in which element material densities were interpolated via the nodal density values (design variables). Guest et al. (2004) introduced nodal design variables and projection schemes into topology optimization to achieve minimum length-scale control and checkerboard-free characteristics. Nodal material densities are regarded as the design variables to calculate the element material densities and element stiffness matrices. Paulino and Le (2009) proposed a kind of hybrid low-order finite elements, in which the nodes for design variable vector are inconsistent with the nodes for displacement vector. Kang and Wang (2011) proposed a nodal density based topology optimization method, in which a non-local Shepard interpolation scheme and higher-order elements are applied to eliminate the numerical instabilities, e.g. the checkerboards.

This paper will propose a multilevel nodal density-based approximation scheme for topology optimization of structures, based on the concept of SIMP method. In this study, regular Q4 (four-node quadrilateral) finite elements are applied to evaluate the displacement field vector, and the nodal densities of each Q4 element are considered as design variables. A family of Shepard functions is employed to implement a non-local density approximant with enhanced smoothness over the entire design domain. At the same time, nodal design variables are used to evaluate practical material properties of the finite elements.

2 Non-local Nodal Density Approximant

The Q4 (4-node quadrilateral) element is considered for all numerical implementations in this paper. A family of Shepard function is used as a non-local approximant to construct a density field with global smoothness over the design space.

2.1 Shepard Function

Let $\phi_i (i = 1, 2, \dots, n_H)$ denote a set of non-negative data values at the associated sampling points $x_i = (X_i, Y_i)$ within the support radius of an arbitrary point. (X_i, Y_i) defines the i th point location in the given Cartesian coordinate system. The approximation of the Shepard function method is stated as

$$\bar{\varphi}(x) = \sum_{i=1}^{n_H} \Theta_i(x) \varphi_i \tag{1}$$

where n_H is the number of the nodes that is within the support radius r of the i th point. The Shepard function $\Theta_i(x)$ is expressed as a normalized formulation

$$\Theta_i(x) = \frac{\omega_i(x - x_i)}{\sum_{j=1}^{n_H} \omega_j(x - x_j)} \tag{2}$$

is the weight function, in the study which is a radially linear ‘hat’ function defined by [Bourdin (2001)], where $x - x_i$ is the radial distance from point x to x_i . Given $D_i(x) = x - x_i = \sqrt{(X - X_i)^2 + (Y - Y_i)^2}$, the weight function can be expressed as

$$\omega_i(x - x_i) = \frac{3}{\pi r^2} \max\left(0, 1 - \frac{D_i(x)}{r}\right) \tag{3}$$

The weight function is zero outside the domain of influential support, and decays linearly with the distance from the interest point x . It means that only nearby points are considered in computing any approximated value. In this way, the cost of computation is greatly saved by eliminating calculations with distant data points. The Shepard function $\Theta_i(x)$ possesses the properties:

$$\sum_{i=1}^{n_H} \Theta_i(x) = 1$$

$$\Theta_i(x) > 0$$

It is apparent that the Shepard function has a mechanism similar to the smoothing effect of the density filtering schemes [Bourdin (2001); Luo, Chen, Yang, Zhang and Abdel-Malek (2005)]. The approximated values via the Shepard function are bounded between lower and upper values of the sampling points, which is essential property for a physically meaningful density field approximant in topology optimization.

2.2 Nodal Density Approximation via the Shepard Function

With the Shepard function method, any nodal density variable relative can be given as

$$\bar{\rho}_n = \sum_{i=1}^{n_H} \Theta_i(x) \rho_i \tag{4}$$

where n_H is the number of nodes within the influence domain. As the indicative scheme given in Fig. 1, “r” is radius of influence domain, and there are five nodes which are considered as the associated points to the concerned n th point.

A physical meaning density approximation in topology optimization should satisfy some basic properties, such as $0 < \rho''$ [Bendsøe and Sigmund (2003)]. The Shepard function approximation can satisfy the non-negative and value-bounded properties. In doing so, the Young’s modulus and elasticity constant on each point can be respectively expressed as

$$\bar{E}_n = (\bar{\rho}_n)^p E_0 = \left(\sum_{i=1}^{n_H} \Theta_i(x) \rho_i \right)^p E_0 \tag{5}$$

$$\bar{D}_n = (\bar{\rho}_n)^p D_0 = \left(\sum_{i=1}^{n_H} \Theta_i(x) \rho_i \right)^p D_0 \tag{6}$$

where E_0 and D_0 are Young’s modulus and elasticity constant of the solid-state material. Following the concept of conventional SIMP approach [Sigmund (2001)], the power-law scheme is used to suppress the intermediate density values in the optimal solution, where p is the penalty factor and is set to 3 in this study.

3 Local Nodal Density Interpolation Scheme

Here, a local nodal density-based interpolation will be presented to convert the nodal design variables into the elemental densities. In this study, the standard Lagrangian shape function in the finite element method is used to interpolate elemen-

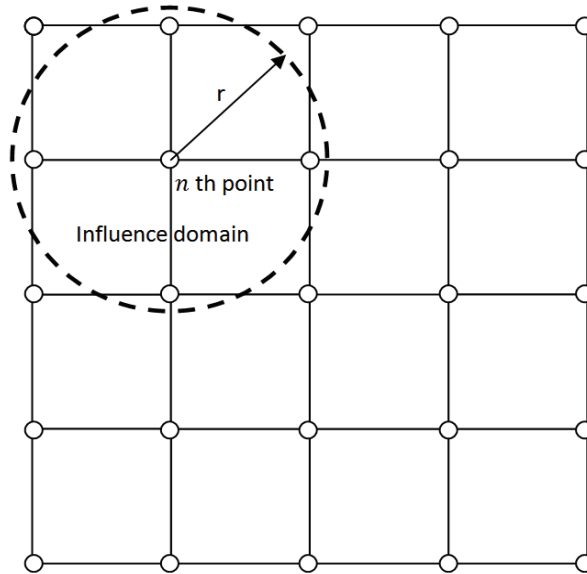


Figure 1: Influence domain of nodal design variable

tal material properties. The local nodal density-based interpolant is stated as

$$\rho_e = \sum_{n=1}^{n_e} N_n \rho'' \quad (7)$$

where ρ_e is the elemental density, n_e is the number of the nodes of each element (4 in Q4 element), and N_n is the standard Lagrangian shape function. For simplicity, 2×2 Gaussian points are utilized to compute the practical material properties and determine the displacement field (Fig. 2).

In the 4-points Gaussian quadrature scheme, the interpolation scheme is expressed as

$$\Phi(\xi, \eta) = \sum_{n=1}^{n_e} N_n(\xi, \eta) \Phi'' \quad (8)$$

where Φ'' denote a set of non-negative data values at the node within each element and n_e equals to 4 in Q4 element. Thus, in Q4 element Eq. (8) can be re-expressed as

$$\Phi(\xi, \eta) = N_1 \Phi'' \quad (9)$$

In Eq. (8) $N_n(\xi, \eta)$ is the standard Lagrangian shape function expressed as

$$N_n(\xi, \eta) = \frac{1}{4} (1 + \xi \xi'') \tag{10}$$

where ξ'' is the local coordinates of 4 nodes in the isoparametric Q4 element, and (ξ, η) represent the coordinates of any Gauss points as shown in Fig. 2.

Furthermore, elemental material properties, such as Young’s modules and elasticity constant, can then be expressed according to the proposed the multi-level approximation scheme, respectively, as

$$E_e = \sum_{n=1}^{n_e} N_n E'' \tag{11}$$

$$\mathbf{D}_e = \sum_{n=1}^{n_e} N_n D'' \tag{12}$$

From the above discussion, it can be found that the proposed multi-level interpolation scheme can be easily implemented and is numerically effective, due to the application of the standard low-order rather than the higher-order finite elements. The obtained nodal variables via the interpolant are bounded between $[0, 1]$, which is crucial for generating a physically meaningful density field.

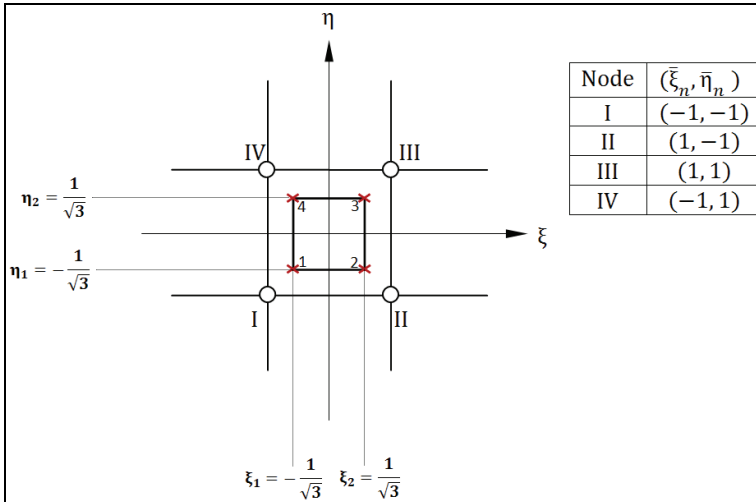


Figure 2: Nodal density variables and the 2×2 Gauss points in finite elements

4 Finite Element Analysis

The regular Q4 (4-node quadrilateral) element is used to determine the displacement field. The density variables located at the corners of Q4 elements are used to represent elemental material properties via Gauss integration. The elemental stiffness matrix can be expressed as

$$\mathbf{K}_e = \int_{\omega_e} \mathbf{B}_e^T \mathbf{D}_e \mathbf{B}_e d\Omega \tag{13}$$

where \mathbf{B}_e is the elemental strain-displacement matrix, \mathbf{D}_e is the elemental elasticity constant matrix and ω_e is the volume occupied by the e th element. Using the 2×2 Gauss numerical integration, the elemental stiffness matrix \mathbf{K}_e can be explicitly expressed by

$$\mathbf{K}_e = \sum_{i=1}^2 \sum_{j=1}^2 [h \mathbf{B}^T(\xi_i, \eta_j) \mathbf{D}(\xi_i, \eta_j) \mathbf{B}(\xi_i, \eta_j) \mathbf{J}(\xi_i, \eta_j) w_i w_j] \tag{14}$$

where $\mathbf{D}(\xi_i, \eta_j)$ is the elasticity constant related to each Gauss point, $\xi_i, \eta_j = \pm 0.5773$, and $w_i, w_j = 1, 1 (i = 1, 2; j = 1, 2)$. w is the corresponding weighting factors and h is the thickness of material.

Considering Eqs. (6) and (12) and using the Gaussian integration, $\mathbf{D}(\xi_i, \eta_j)$ can be expressed as follows:

$$\mathbf{D}(\xi_i, \eta_j) = \sum_{n=1}^{n_e} N_n(\xi_i, \eta_j) \mathbf{D}'' \tag{15}$$

Thus, the stiffness matrix of the finite element can be $w_i, w_j = 1, 1 (i = 1, 2; j = 1, 2)$ explicitly given by

$$\mathbf{K}_e = \sum_{i=1}^2 \sum_{j=1}^2 \left[h \mathbf{B}^T(\xi_i, \eta_j) \left(\sum_{n=1}^{n_e} [N_n(\xi_i, \eta_j) \left(\sum_{i=1}^{n_H} \Theta_i(x_n) \rho_i \right)^P D_0] \right) \mathbf{B}(\xi_i, \eta_j) \mathbf{J}(\xi_i, \eta_j) w_i w_j \right] \tag{16}$$

where N_n is the standard Lagrangian shape function shown, and n_e is the number of nodes in each element and equals to 4 here. Θ_i is the Shepard function and ρ_i is the density value at the i th elemental node. x_n is the coordinates of n th node in each element.

5 Topology Optimization Problem

Structural mean compliance design [Bendsøe and Sigmund (2003)] is employed as the topology optimization problem, due to its well-established theory and conceptual simplicity

$$\begin{aligned} \text{Minimize: } J &= \mathbf{U}^T \mathbf{K} \mathbf{U} = \sum_{e=1}^{N_e} (\rho_e)^p \mathbf{u}_e^T \mathbf{k}_e \mathbf{u}_e \\ \text{Subject to: } &\begin{cases} V - f_v V_0 \leq 1 \\ \rho_{\min} \leq \rho_e \leq 1 \\ \mathbf{K} \mathbf{U} = \mathbf{F} \end{cases} \end{aligned} \tag{17}$$

where the objective function j is to be minimized, \mathbf{U} is the displacement vector and \mathbf{K} is the global stiffness matrix, \mathbf{F} is the external vector. N_e is the number of total elements, \mathbf{u}_e is the elemental displacement vector, and \mathbf{k}_e is the elemental stiffness matrix. p is the penalty factor ($p = 3$ in this study). V is the actual material volume and f_v is the specified volume fraction ratio, and V_0 is the volume of the design domain. $\rho_{\min} = 0.0001$ is the lower bound of elemental densities to avoid singularity in numerical implementation.

The derivative of the objective function with respect to the nodal design variables is expressed as

$$\frac{\partial j(\rho_i)}{\partial \rho_i} = -\mathbf{U}^T \frac{\partial \mathbf{K}}{\partial \rho_i} \mathbf{U} = -\sum_{e \in n_i} \mathbf{u}_e^T \frac{\partial \mathbf{k}_e}{\partial \rho_i} \mathbf{u}_e \tag{18}$$

where n_i is an index set containing indices of all the elements connected to the th point. The derivative of the elemental stiffness matrix $\partial \mathbf{k}_e / \partial \rho_i$ can be obtained as below

$$\begin{aligned} \frac{\partial \mathbf{k}_e}{\partial \rho_i} &= \sum_{i=1}^2 \sum_{j=1}^2 \left[h \mathbf{B}^T(\xi_i, \eta_j) \left(\sum_{n=1}^{n_e} [N_n(\xi_i, \eta_j)] p \left(\sum_{i=1}^{n_H} \Theta_i(x_n) \rho_i \right)^{(p-1)} D_0 \right) \right. \\ &\quad \left. \mathbf{B}(\xi_i, \eta_j) \mathbf{J}(\xi_i, \eta_j) w_i w_j \right] \end{aligned} \tag{19}$$

6 Numerical Examples and Discussions

Three typical numerical examples, namely, cantilever beam, MBB beam and Mitchell-type structure, are used to demonstrate the effectiveness of the proposed multi-level approximation scheme. For the “artificial” material model, Young’s modulus for solid material is 1 and Poisson’s ratio is 0.3, the volume constraint is taken as 50%.

In the study, the set of nodal densities serve as the design variables of the topology optimization. There is no sensitivity filtering applied and the radius of support domain is set to 2.0. For the comparison purpose, the elemental-based SIMP method [Sigmund (2001)] is implemented with different mesh refinements, with and without using the sensitivity filtering scheme, respectively. The convergence criterion is the relative error between two adjacent iterations less than 0.005.

6.1 Cantilever beam

Fig.4 is the design domain of the cantilever beam with an aspect ratio of 2:1 corresponding to length over height. The left side of the domain is fixed as the Dirichlet boundary while the right side is treated as a non-homogenous Neumann boundary with a concentrated force $F=1$, vertically applied at the centre point. The objective function is to minimize the mean compliance. As shown in Fig.5, the design domain is discretized with $100 \times 50 = 5000$ finite elements and the design variables nodal density variables.

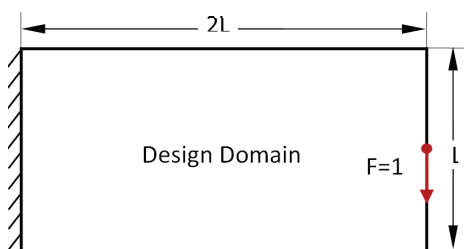


Figure 4: Design domain of the cantilever beam

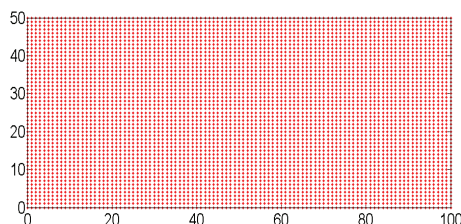


Figure 5: FE nodes in the design domain

The topology optimization is converged after 319 iterations, and the overall structural mean compliance is minimized from 319.136 to 66.519. Fig.6 shows the discrete plots of the nodal densities at different design stages, in which the first figure is the initial design, the last figure is the optimal design, and the rest are the intermediate designs. The corresponding contours of the design variables are displayed in Fig.7 that shows the design gradually moves towards the lower limit 0.0001 (weak material) and upper limit 1 (solid material) during the optimization. So it can be seen that the topology optimization in this study can actually be regarded as a numerically iterative process to re-distribute a number of material density points in the design space until the convergence criterion is satisfied.

Fig.8 displays the topology plots of the element stiffness at different design stages of the optimization. The optimization using the proposed nodal density-based

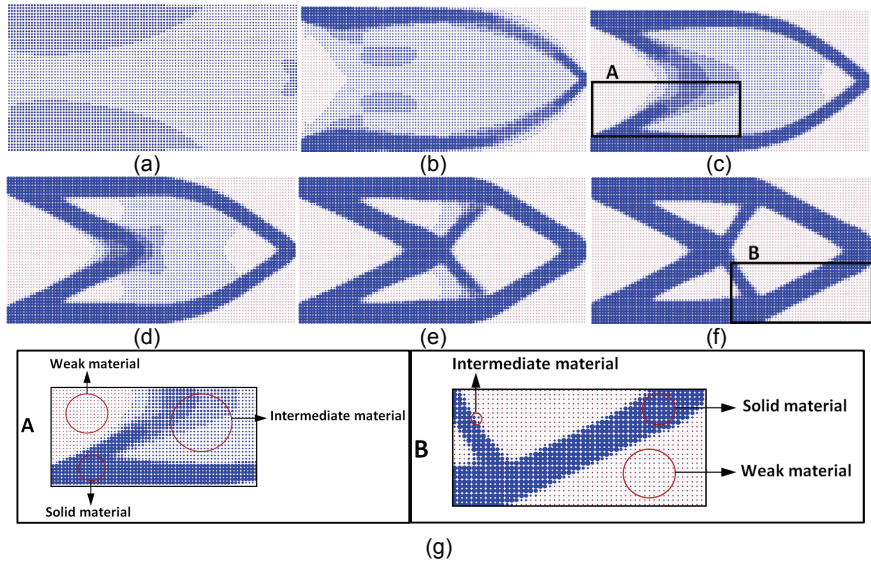


Figure 6: Topology plots: (a) initial design, (b)-(e) intermediate designs, and (f) final solution, the size of the node denoting the magnitude of nodal density values. (g) Local zoom-out plots

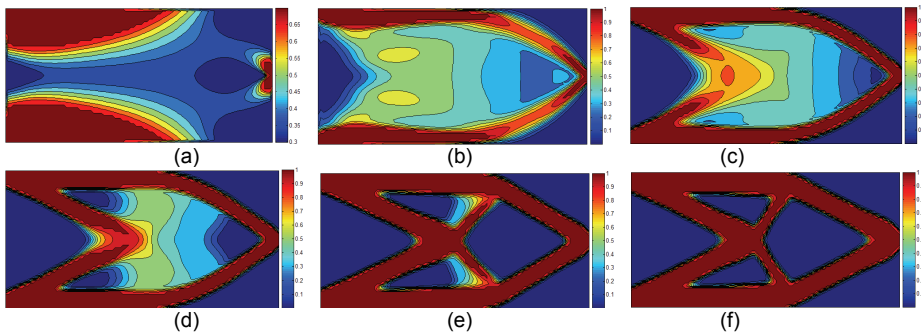


Figure 7: Contour plots of nodal design variables (a) initial design, (b)-(e) intermediate designs, and (f) final solution

method can result in checkerboard-free design, and the so-called “layering” or “islanding” numerical phenomenon [Rahmatalla and Swan (2004)] can also be eliminated by using the present Shepard function approximant. Table 1 displays the topological plots related to different mesh refinement levels (60×30 , 80×40 , 100×50),

using the proposed method and conventional SIMP method, with and without sensitivity filtering scheme [Sigmund (2001)], respectively. It can be seen that the results obtained by conventional SIMP method without using the sensitivity filtering scheme suffer from the checkerboards and “islanding” phenomenon. These numerical instabilities can be eliminated by using the conventional SIMP method with the sensitivity filtering scheme. However, the element-wise SIMP may give rise to the mesh-dependency. In contrast to the conventional SIMP method, the proposed point-wise Shepard function method can achieve checkerboard-free and mesh independent designs, without applying any sensitivity filtering schemes.

Figure 9 shows curves of the objective function and the volume constraint over the iterations. It is noted that the first 75 iterations are mainly employed to implement topological optimization, and the rest iterations are used to adjust local structural shapes until a uniform distribution of the strain energy in the structure is achieved. Since the proposed method has been proved to be mesh-independent, it is possible to use a coarser finite element mesh to improve computational efficiency. According to the curve of constraint, the proposed method is well mass conservative.

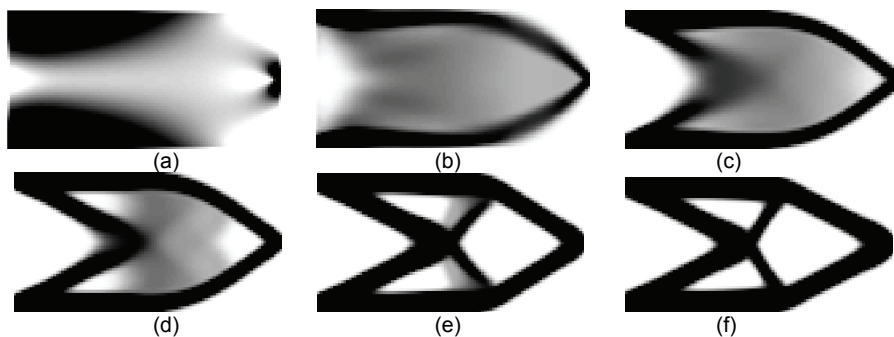
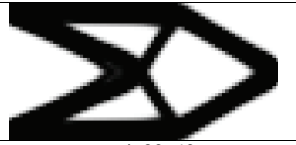
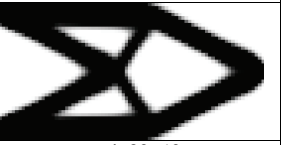


Figure 8: Topology plots of point-wise nodal design variables: (a) initial design, (b)-(e) intermediate designs, and (f) final solution

6.2 MBB beam

The MBB beam is studied as the second numerical example. The beam has an aspect ratio of 6:1 having regard to the length over height. Only half of the beam is modelled in the numerical implementation, due to the symmetry of the MBB beam. As shown in Fig. 10, a vertically force $F=1$ is applied at the top-left corner of the MBB structure and the bottom-right corner is simply supported. The design domain is discretized with $120 \times 40 = 4800$ Q4 elements, and the nodal design variables in the design domain are shown in Fig. 11.

Table 1: Results of different meshes

Elemental density-based method without sensitivity filtering	Elemental density-based method with sensitivity filtering	Nodal density-based method without sensitivity filtering
 mesh 60×30	 mesh 60×30	 mesh 60×30
 mesh 80×40	 mesh 80×40	 mesh 80×40
 mesh 100×50	 mesh 100×50	 mesh 100×50

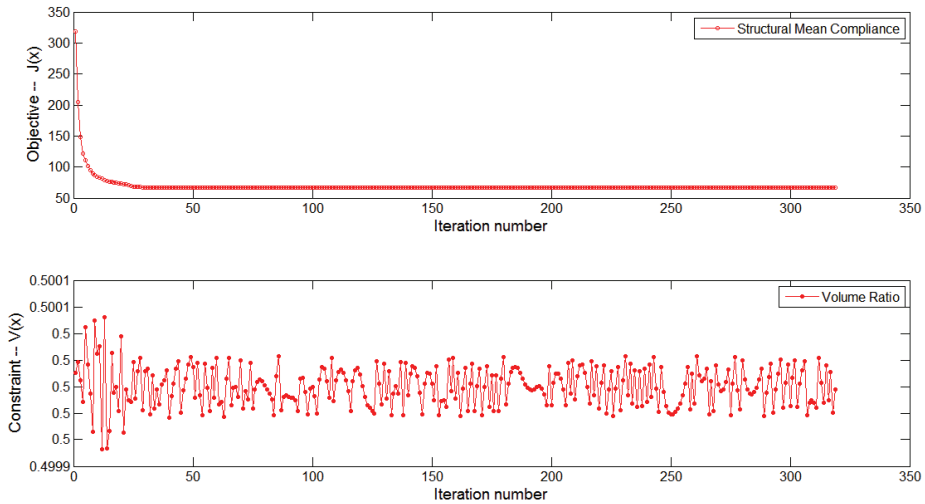


Figure 9: Iteration histories of objective function and volume constraint

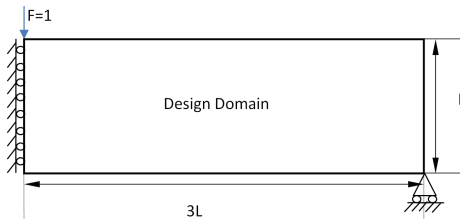


Figure 10: Design domain for the half of MBB beam

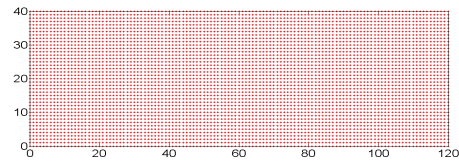


Figure 11: FE nodes in the design domain

Table 2: Results of different meshes

Elemental density-based method without sensitivity filtering	Elemental density-based method with sensitivity filtering	Nodal density-based method without sensitivity filtering
		
mesh 60×20	mesh 60×20	mesh 60×20
		
mesh 90×30	mesh 90×30	mesh 90×30
		
mesh 120×40	mesh 120×40	mesh 120×40

The design is converged after 245 iterations, with the overall strain energy being minimized from 1026.843 to 204.689. Fig. 12 shows the discrete plots of the nodal densities, while the Fig. 13 displays the contour plots of the nodal densities. It can be seen that the nodal density field is gradually converges to the lower and upper bounds of the design variables (0.0001 and 1), which are used to indicate the weakness and solid material phases in the design domain, respectively. So we can see that the proposed SIMP-based topology optimization is actually an iterative process to re-distribute a number of point-wise nodal density variables in the design domain until the design approaches toward a so-called “0-1” binary distribution. The grey-level topological plots based on the nodal variables are given in Fig. 14, which shows that the optimal design can be obtained via the topological change of structure. The above results show that the proposed nodal density-based methodology is actually a checkerboard-free topology optimization approach, which can also eliminate “layering” or “islanding” phenomenon by using the Shepard density approximant.

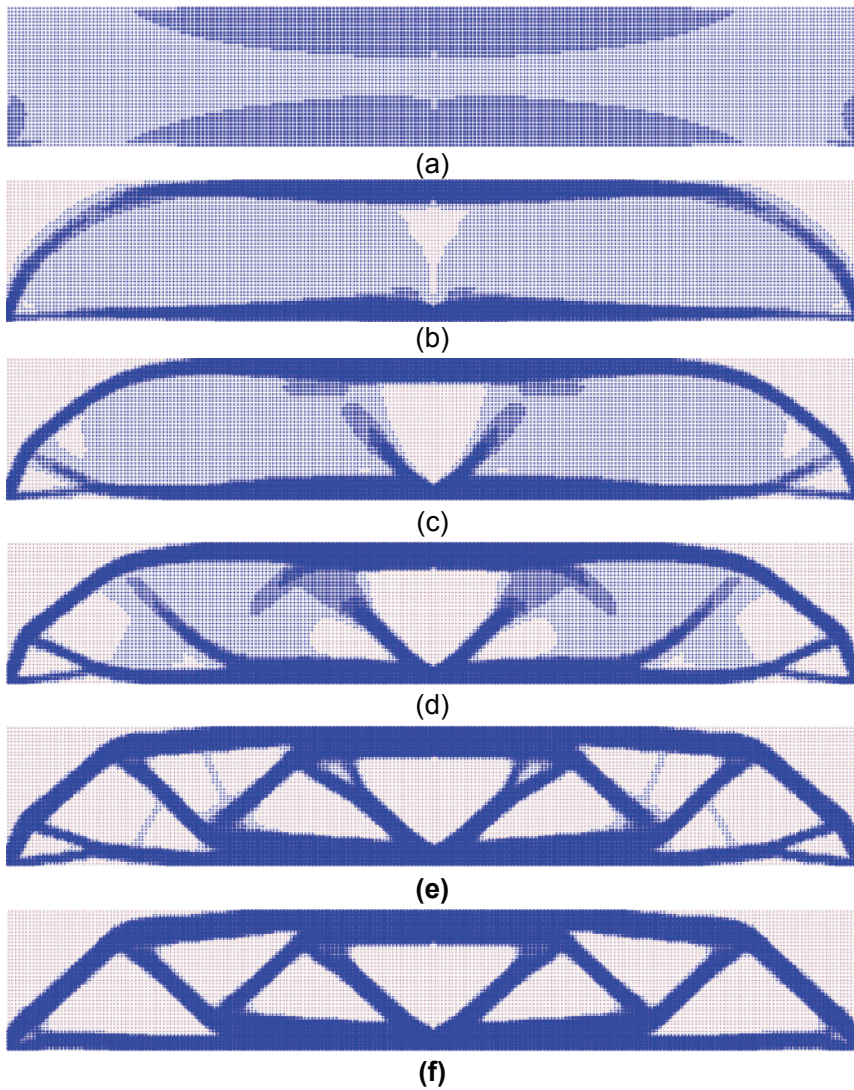


Figure 12: Nodal plots of nodal material densities: (a-e) intermediate results, and (f) final solution.

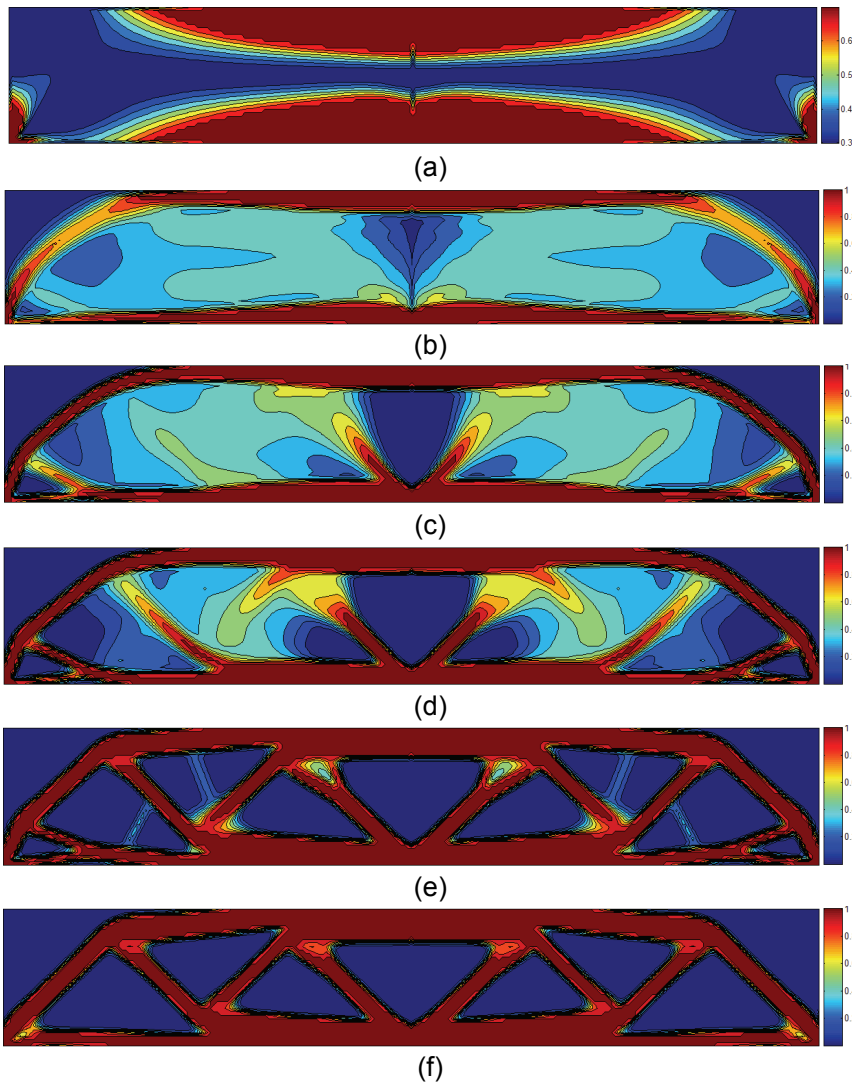


Figure 13: Contour plots of nodal material densities: (a-e) intermediate results, and (f) final solution.

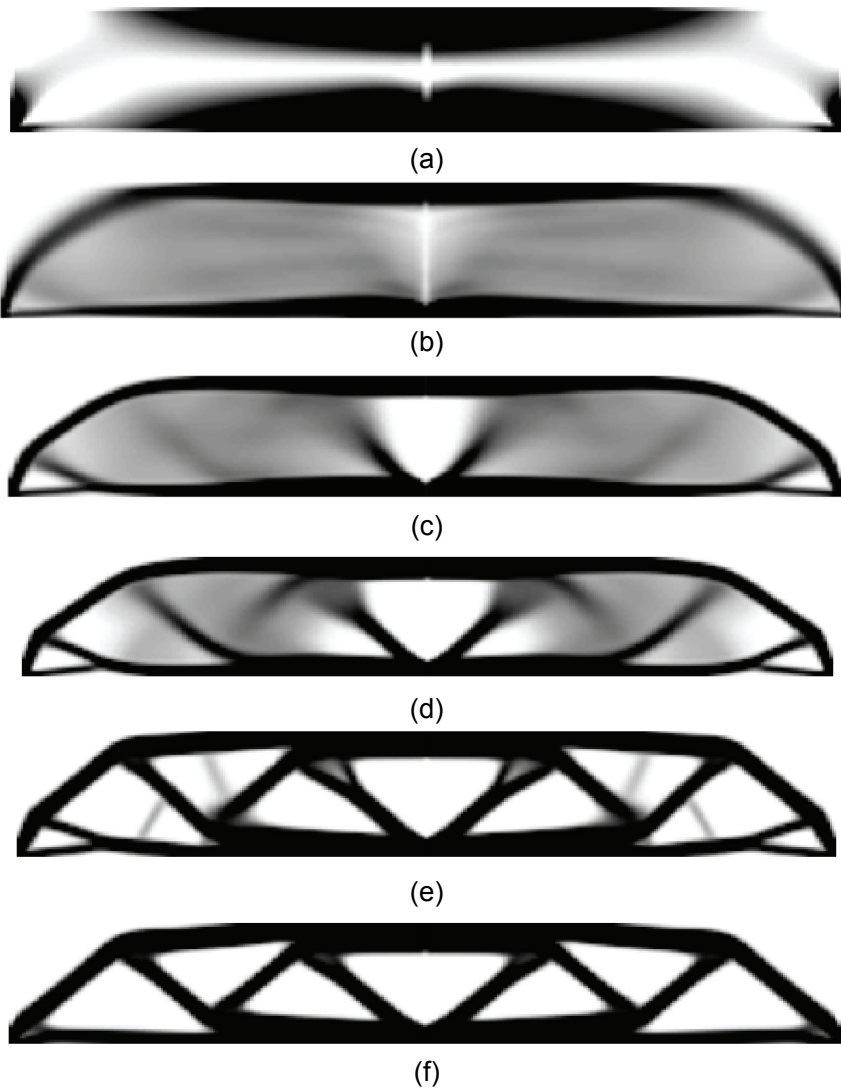


Figure 14: Topology plots of point-wise nodal design variables: (a-e) intermediate results, and (f) final solution.

To compare the proposed nodal SIMP method with the conventional elemental-based SIMP method, three different meshing refinements, namely, $60 \times 20 = 1200$, $90 \times 30 = 2700$, and $120 \times 40 = 4800$, are applied to the conventional elemental SIMP method, by using and without using the sensitivity filtering scheme [Sigmund (2001)], respectively. And these meshing refinements are then applied to the proposed nodal SIMP method. As seen in Table 2, for the conventional SIMP method, the results without sensitivity filtering suffer from the checkerboard patterns and “islanding” phenomenon, while the designs with the sensitivity filtering do not subject to the checkerboard patterns and “islanding” phenomenon. However, this element-wise SIMP scheme will give rise to the mesh-dependency. From the results, it can be found that the proposed nodal density SIMP method can eliminate checkerboard patterns and “islanding” phenomenon, as well as the mesh-dependency without using any density and sensitivity filtering techniques. Fig. 15 displays the curves of the objective function and volume constraint over the iterations. It can be seen that the whole iterations are used to achieve a uniform distribution of the strain energy in the structure for satisfying the optimal criteria and the volume constraint is mass conservative.

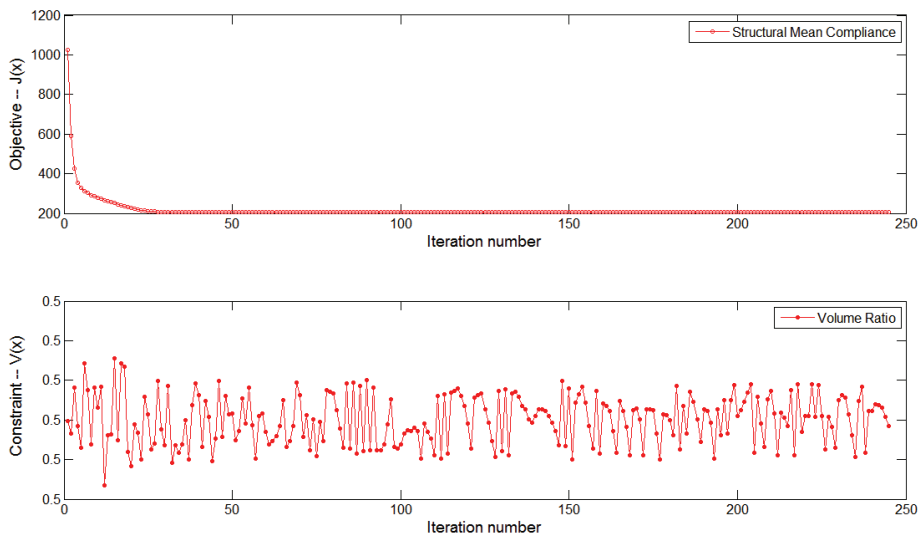


Figure 15: Iteration histories of objective function and volume constraint

6.3 Mitchell-type structure

Fig. 16 is the design domain of the Mitchell-type structure with an aspect ratio of 2:1 with respect to the length over height, and a concentrated force $F=1$ is vertically applied at the model point of its lower edge. The objective function is to minimize the mean compliance. As shown in Fig. 17, the design domain is discretized with $100 \times 50 = 5000$ elements and the design variables are the nodal variables.

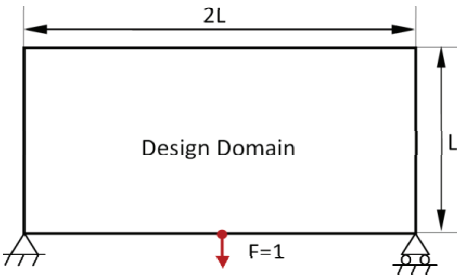


Figure 16: Design domain

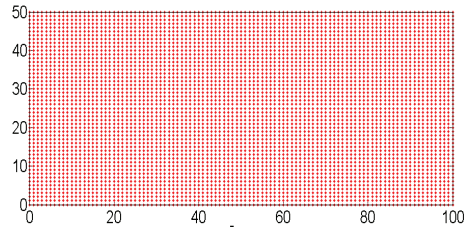


Figure 17: FE nodes in the design domain

The topological optimization is converged after 174 iterations, and the overall structural mean compliance is minimized from 81.819 to 15.208. Fig. 18 shows the discrete plots of the nodal densities at different design stages, which show that the nodal density-based variables can be applied to describe topologies of the structure. The contour plots of the design variables are displayed in Fig.19, which shows, following the optimization process, the design variables are gradually pushed towards the lower limit 0.0001 (weak material) and upper limit 1 (solid material). Fig. 20 showcases the nodal density-based topological plots corresponding to the different steps. The results again evidence that the proposed SIMP method is a checkerboard-free approach. At the same time, with the Shepard approximation scheme, the “layering” or “islanding” phenomenon is also eliminated in this study.

Table 3 shows the optimal topologies corresponding to different finite element meshes ($60 \times 30 = 1800$, $80 \times 40 = 3200$ and $100 \times 50 = 5000$) using the proposed SIMP method and conventional SIMP method (with and without sensitivity filtering scheme), respectively. From the results, it can be easily found that the checkerboard patterns and “islanding” phenomenon will occur in the designs obtained via the conventional SIMP method without using the sensitivity filtering scheme, while the conventional SIMP method using the sensitivity filtering scheme can generate checkerboard-free designs. However, the element-wise SIMP scheme may subject to the mesh-dependency, when applied to the same design with a mesh refinement. With regard to the proposed SIMP method, despite the refinement of meshes, the topolo-

gies of structure remain unchanged, which denotes the proposed SIMP model based on the Shepard function approximant is mesh independent. Moreover, this method can also eliminate checkerboard patterns and “islanding” phenomenon without using any filtering schemes.

It is noted that the iteration numbers will vary having regard to a refinement of the finite element meshes. The mesh independence of the proposed method provides a way to employ a relatively coarser mesh in the numerical implementation, to make the computation more cost-effective. Figure 21 gives the curves of the objective function and volume constraint over the iterations, in which the curve of constraint denotes that the proposed method is well mass conservative.

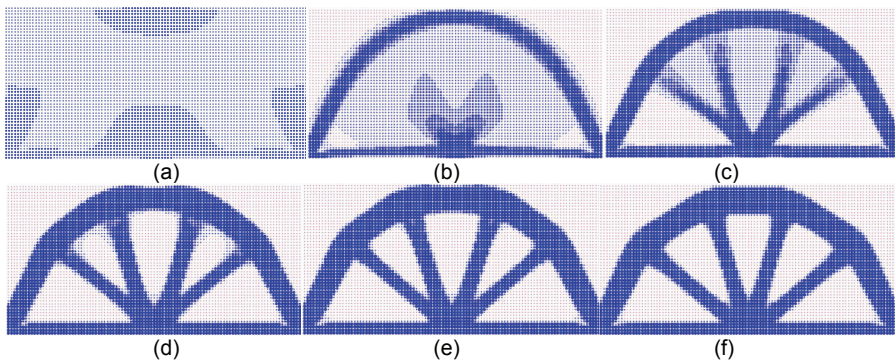


Figure 18: Topology plots of point-wise nodal material densities: (a-e) intermediate results, and (f) final solution.

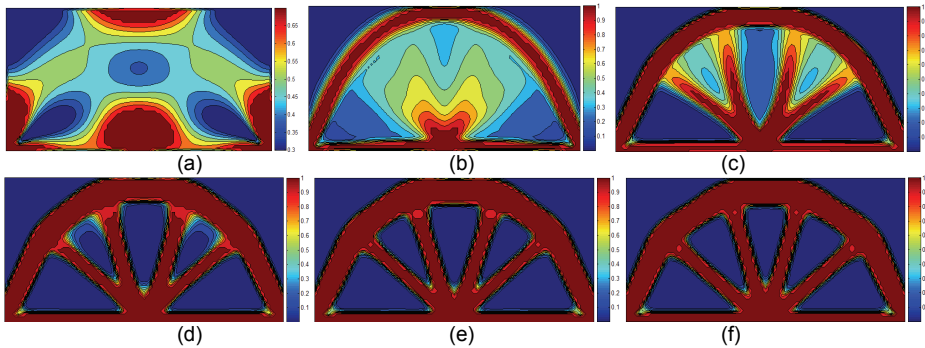


Figure 19: Contour plots of point-wise nodal design variables

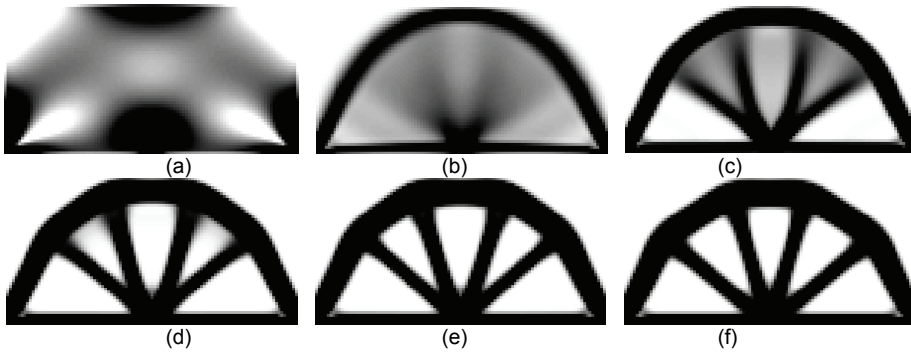


Figure 20: Topology plots of point-wise nodal design variables: (a-e) intermediate results, and (f) final solution.

Table 3: Results of different meshes

Elemental density-based method without sensitivity filtering	Elemental density-based method with sensitivity filtering	Nodal density-based method without sensitivity filtering
 mesh 60×30	 mesh 60×30	 mesh 60×30
 mesh 80×40	 mesh 80×40	 mesh 80×40
 mesh 100×50	 mesh 100×50	 mesh 100×50

7 Conclusions

In this paper, an alternative SIMP scheme is proposed for topological optimization of structures based on a multi-level Shepard function approximant. In this

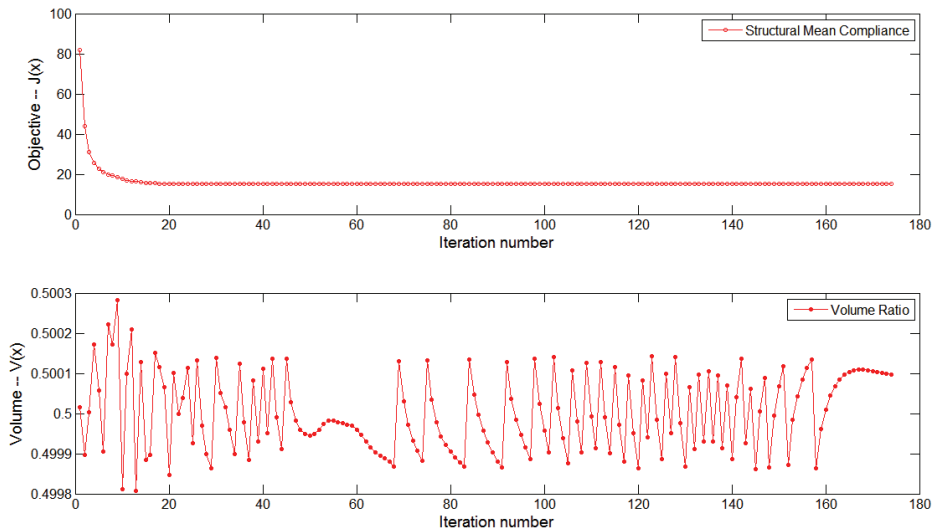


Figure 21: Iteration histories of objective function and volume constraint

method, the nodal variables are considered as the design variables, to implement structural topology changes. A nodal density field with enhanced smoothness is constructed by using the original set of design variables via a non-local Shepard function method. The new set of nodal variables is applied to evaluate the practical material properties of finite elements, via a local interpolation scheme of the standard Lagrangian shape function. Therefore, instead of using the time-consuming higher-order elements, the lower-order finite elements can be easily employed to improve computational efficiency. The proposed topology optimization methodology is able to eliminate the typical numerical instabilities in the topology optimization of continuum structures. It is straightforward to extend the proposed multi-level topology optimization method to more advanced mechanics problems.

Acknowledgement: The research is partially supported by National “973” Project of China (2010CB328005), Key Project of National-Science-Foundation of China (60635020), and Chancellor’s Research Fellowship (University of Technology, Sydney), and Australian Research Council, Discovery projects: DP1094451 and DP09-88429.

References

- Allaire, G., Jouve, F., Toader, A.M.** (2004): Structural optimization using sensitivity analysis and a level-set method, *Journal of Computational Physics*, vol. 194, pp. 363-393.
- Bendsøe, M.P., Kikuchi, N.** (1988): Generating optimal topologies in structural design using a homogenization method, *Computer Methods in Applied Mechanics and Engineering*, vol. 71, pp. 197-224.
- Bendsøe, M.P., Sigmund, O.** (1999): Material interpolation schemes in topology optimization, *Archive of Applied Mechanics*, vol.69, pp. 635-654.
- Bendsøe, M.P., Sigmund, O.** (2003): *Topology optimization: Theory, Methods, and Applications*, Springer, Berlin Heidelberg.
- Bourdin, B.** (2001): Filters in topology optimization, *International Journal for Numerical Methods in Engineering*, vol. 50, pp. 2143-2158.
- Diaz AR, Sigmund O.** (1995): Checkerboard patterns in layout optimization, *Structural and Multidisciplinary Optimization*, vol. 10, pp. 40-45.
- Guest, J.K., Prevest, J.H., Belytschko, T.** (2004): Achieving minimum length scale in topology optimization using nodal design variables and projection functions. *International Journal for Numerical Methods in Engineering*, vol. 61, pp. 238-254.
- Kang, Z., Wang, Y.** (2011): Structural topology optimization based on non-local Shepard interpolation of density field, *Computer Methods in Applied Mechanics and Engineering*, vol. 200, pp. 3515–3525.
- Li, S., Atluri, S.N.** (2008): The MLPG mixed collocation method for material orientation and topology optimization of anisotropic solids and structures, *CMES-Computer Modeling in Engineering & Sciences*, vol. 30, pp. 37-56.
- Luo, Z., Chen, L.P., Yang, J.Z., Zhang, Y.Q., Abdel-Malek, K.** (2005): Compliant mechanism design using multi-objective topology optimization scheme of continuum structures, *Structural and Multidisciplinary Optimization*, vol. 30, pp. 142–154.
- Luo, Z., Wang, M.Y., Wang, S.Y., Wei, P.** (2008): A level set-based parameterization method for shape and topology optimization, *International Journal for Numerical Methods in Engineering*, vol. 76, pp. 1-26.
- Luo, Z., Zhang, N., Gao, W., Ma, H.** (2012) Structural shape and topology optimization using a meshless Galerkin level set method, *International Journal for Numerical Methods in Engineering*, vol. 90, pp. 369-389.
- Luo, Z., Zhang, N., Wang, Y.** (2012): A physically meaningful level set method

for topology optimization of structures, *CMES-Computer Modeling in Engineering & Sciences*, vol.83, pp.73-96.

Matsui, K., Terada, K. (2004): Continuous approximation of material distribution for topology optimization. *International Journal for Numerical Methods in Engineering*, vol. 59, pp. 1925-1944.

Mlejnek, H.P. (1992): Some aspects of the genesis of structures, *Structural Optimization*, vol. 5, pp. 64-69.

Paulino, G.H., Le, C.H. (2009): modified Q4/Q4 element for topology optimization, *Structural and Multidisciplinary Optimization*, vol. 37, pp. 255-264.

Rahmatalla, S.F., Swan, C.C. (2004): A Q4/Q4 continuum structural topology optimization implementation, *Structural and Multidisciplinary Optimization*, vol. 27, pp. 130-135.

Sethian, J.A., Wiegmann, A. (2000): Structural boundary design via level set and immersed interface methods, *Journal of Computational Physics*, vol. 163, pp. 489-528.

Sigmund, O., Petersson, J. (1998): Numerical instabilities in topology optimization: a survey on procedures dealing with checkerboards, mesh-dependency and local minima, *Structural and Multidisciplinary Optimization*, vol. 16, pp. 68-75.

Sigmund, O. (2001): A 99 topology optimization code written in Matlab, *Structural and multidisciplinary optimization*, vol. 21, pp. 120-127

Wang, M.Y., Wang, X.M., Guo, D.M. (2003): A level set method for structural topology optimization, *Computer Methods in Applied Mechanics and Engineering*, vol. 192, pp. 227-246.

Zhou, M., Rozvany, G.I.N. (1991): The COC algorithm, Part II: topological, geometry and generalized shape optimization, *Computer Methods in Applied Mechanics and Engineering*, vol. 89, pp. 197-224.

Zheng, J., Long, S.Y., Xiong, Y., Li, G.Y. (2008): A topology optimization design for the continuum structure based on the meshless numerical technique, *CMES-Computer Modeling in Engineering & Sciences*, vol. 29, pp. 137-154.